

ACOUSTIC VISION WITH THE NONLINEAR TECHNIQUES

IGOR DIDENKULOV

Institute of Applied Physics
46 Ulyanov Str., Nizhny Novgorod, 603950, Russia
din@hydro.appl.sci-nnov.ru

Nonlinear acoustic methods are found increasing applications during the last decades. They are effective for diagnostics of bubbles in liquids and cracks in solids since bubbles and cracks are strongly nonlinear scatterers. In this paper the nonlinear acoustic techniques for imaging of liquids and solids with the nonlinear acoustic defects are described. Results of investigation demonstrate possibilities of the nonlinear acoustic techniques in nondestructive testing of different media.

INTRODUCTION

Acoustic methods of nondestructive testing (NDT) are widely used in industries and science. Traditional acoustic NDT methods which are known for many decades are based on measurement of linear acoustic parameters: sound velocity, attenuation. Methods of acoustic imaging have also been elaborated for quite a long time. They are mainly based on the use of linearly scattered waves from an object and widely used in medicine.

Some objects, such as gas bubbles in fluids [1-7] or cracks in solids [8-16], are known to have strongly nonlinear acoustic responses. Different nonlinear acoustic methods are used to detect such objects with highly nonlinear responses [3-6]. But it was mainly investigated the detection of small-size nonlinear inhomogeneities compared to the wavelengths. If the size of an object is large compared to the wavelength, methods of nonlinear acoustic imaging can be employed. In the first part of this paper we describe a method of acoustic vision based on the use of combination acoustic scattering for such large-size objects.

The nonlinear acoustic parameters of solids are much more sensitive to crack-like defects than the linear acoustic parameters (sound velocity, attenuation). Crack can produce different nonlinear acoustic responses such as higher harmonics generation or frequency mixing when ultrasound waves of different frequencies pass through or reflected from a crack and some others. These effects are used for development of the methods of nonlinear acoustic nondestructive testing [8-16]. Simple techniques can be used for detection of damaged objects. However, such techniques cannot give information on crack location. Advanced

methods allow one to find crack position - crack vision [17-20]. In the second part of this paper we present results on crack vision with the nonlinear acoustic pulse techniques and the nonlinear acoustic tomography techniques.

1. THE DIFFERENCE-FREQUENCY ACOUSTIC VISION

The difference-frequency technique is based on registration of the difference frequency wave scattered by the nonlinear scattering object which is illuminated with two high-frequency primary waves [1,3,4]. The experiments were carried out in a water tank [7]. Steel cylinders were chosen to be the observed objects. They were vertically arranged and have diameter 40 mm and length 300 mm spaced 20 cm apart. Acoustic images were constructed by line-angular scanning of sonar with a spherical mirror. The cylinders were sounded by two noncollinear CW ultrasonic beams at 195 kHz and 130 kHz. The cylinder surfaces were covered by gas electrolysis microbubbles to produce highly nonlinear scattering from the surfaces at higher harmonics and the combination frequencies. In the experiment we registered the difference-frequency scattering. A spherical receiving mirror 35 cm in diameter with focus distance of 27.5 cm was made of foam plastic. A synchro-drive provided angular scanning. Signals focused by the mirror on detection were registered by an ADC, fed to a computer, and the image was displayed on the monitor.

The geometry of the experiment is shown in Fig. 1, where 1 and 2 are cylinders, 3 and 4 are emitters ($f_1=195$ kHz, $f_2=130$ kHz), 5 is a receiving hydrophone, 6 is a spherical mirror, and 7 is a computer. The distance between the mirror and the cylinders was 2 m.

A synthesized image of two cylinders at the difference frequency of 65 kHz is shown in Fig. 2.

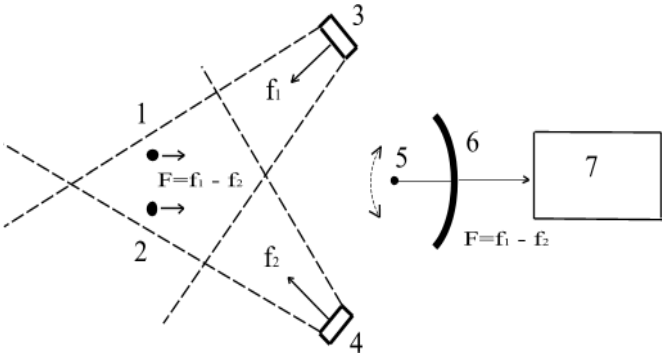


Fig. 1. A scheme of the experiment

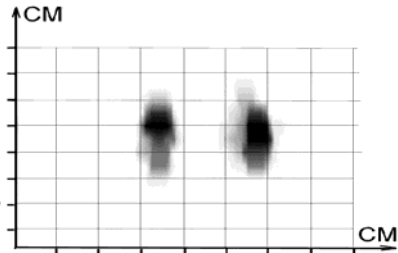


Fig. 2. An image of two metal cylinders obtained at the difference frequency 65 kHz

The images of cylinders were also obtained at the primary frequencies due to linear scattering of primary high frequency waves by the objects. A section of the image along one horizontal line obtained in the linear regime at a high primary frequency is shown in Fig. 3. Figure 4 presents a section along the same horizontal line of the image shown in Fig. 2 at the difference frequency of 65 kHz. For comparison figures 3 and 4 are placed together and the values of amplitudes given along the vertical axes were normalized to unity. One can see from figures 3 and 4, that the image in the nonlinear regime is more contrast compared to the linear one. The nonlinear regime provides also better spatial resolution.

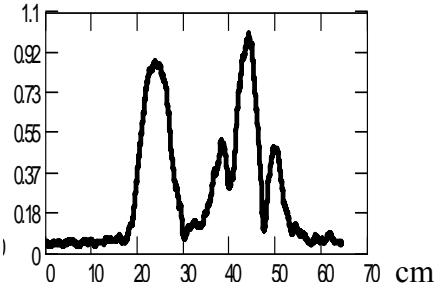


Fig.3. A section of the image of two metal cylinders covered with electrolysis bubbles along one horizontal line obtained by the linear scattering at a high primary frequency 195 kHz. Amplitudes along the vertical axis are normalized to unity

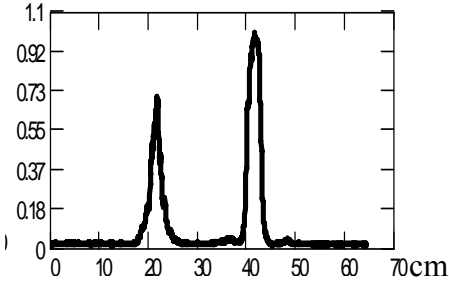


Fig.4. A section of the image of two metal cylinders covered with electrolysis bubbles along one horizontal line obtained at the difference frequency 65 kHz. Amplitudes along the vertical axis are normalized to unity

Experiment on obtaining of an image of a turbulent water jet with air bubbles was done in a water tank. A turbulent water jet was ejected from the cylindrical nozzle at the depth of about 0.5 m from the water surface. A scheme of the experiment is shown in figure 5.

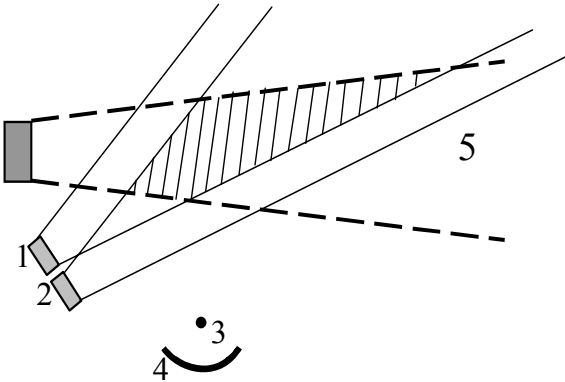


Fig.5. A scheme of experiment. 1 and 2 are primary acoustic wave transducers. 3 – hydrophone, 4 – spherical mirror, 5 – turbulent water jet with bubbles ejected by a nozzle

A jet was insonified by two ultrasonic beams (1 and 2 in the figure 5) having frequencies 132 kHz and 195 kHz, respectively. Sound scatterers – bubbles are generated by

hydrodynamic cavitation process near the nozzle and are taken by the jet down the flow. The difference frequency 63 kHz signal scattered from the jet is received by the focusing receiving system. The focusing system allow one to register the scattered wave near the focal point of the system. It consists of the hydrophone 3 and the spherical mirror 4 made of porous plastic material providing approximately the free-boundary condition at the mirror surface (about -1 value of the reflection coefficient). The receiving system can be moved in horizontal and vertical plane automatically. The difference frequency signal after filtration and amplification is input into computer.

Results of experiments are shown in figure 6. It is a plane and 3D-representation of an image of the jet with bubbles. X-coordinate corresponds to the jet axis, while Y-coordinate is perpendicular to the jet axis. From the figure 6 one can see the main features of the jet: the jet width increases down the flow and there are fluctuations of the bubble density in the jet due to the turbulence.

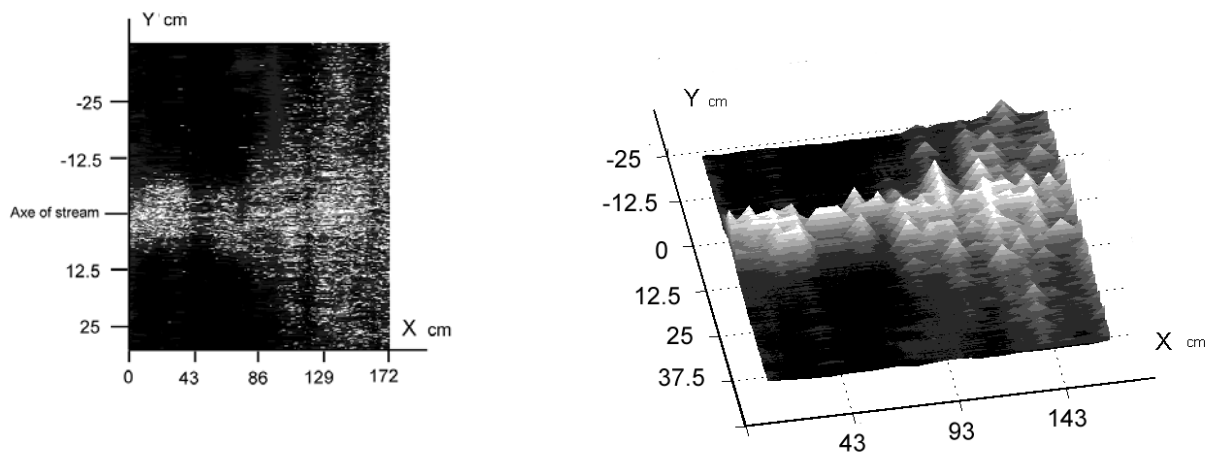


Fig.6. Plane (left) and 3D-representation (right) representation of an image the turbulent jet with gas bubbles obtained at the difference frequency 63 kHz. X-coordinate is along the jet axis, and Y – perpendicular to the jet

2. NONLINEAR ACOUSTIC VISION OF CRACK-LIKE DEFECTS IN SOLIDS WITH PULSE TECHNIQUES

Since a crack is the highly nonlinear acoustic object the nonlinear methods can be employed for crack detection. One of the most effective methods is the modulation one. The modulation method is based on the effect of modulation of high-frequency acoustic wave passing through a crack by low-frequency oscillations of testing samples. Low-frequency wave changes parameters of the high-frequency probe wave propagating through the crack.

Crack location methods can be based on combination of pulse and modulation techniques - modulation of acoustic pulses reflected from a crack by vibrations [17,18]. The first method, i.e. the **pulse modulation technique** employs the modulation of a single ultrasound pulse by vibration of the sample. A scheme of the single pulse modulation method of crack location is shown in Fig. 7 (left). Two signals - high-frequency (HF) tone-burst acoustic pulse of carrier frequency f and low-frequency (LF) CW acoustic wave of frequency F are simultaneously input into the sample. Reflected from crack HF pulse is received and analyzed. Acoustic nonlinearity of a crack results in nonlinear interaction of HF

and LF waves at the crack and the combination frequencies $f_r = nf \pm mF$ ($n, m = 1, 2, \dots$) arise in the reflected signal. Acoustically linear defects can not produce nonlinear responses. It makes possible to identify reflections from cracks among others. The distance r from the HF transducer to the crack can be obtained from pulse travel time t : $r = ct/2$, with the spatial resolution $\Delta r = c\tau/2$ (c is the sound velocity). The travel time can be measured by strobing of the receiving signal with the known time delay. To detect single pulse modulation the pulse duration τ must satisfy the relation $F\tau > 1$.



Fig.7. Schemes of single pulse (left) and pulse train (right) techniques of crack location

This method was tested in experiments with aluminium and steel rods of 1.4 m length. Artificial crack was made at 50 cm from the rod end with HF ($f=570$ kHz, $\tau = 60 \mu\text{s}$) transducer. Receiving sensor was attached to the rod wall at 25 cm from the first transducer, so that the total round trip path for acoustic pulse was 75 cm. Low frequency 70 kHz transducer was attached to the opposite end of the rod. One of experimental results is shown in Fig. 8. It is spectra of received signal made with time shift of $5 \mu\text{s}$ from each other within the pulse round trip time interval from 140 to $185 \mu\text{s}$.

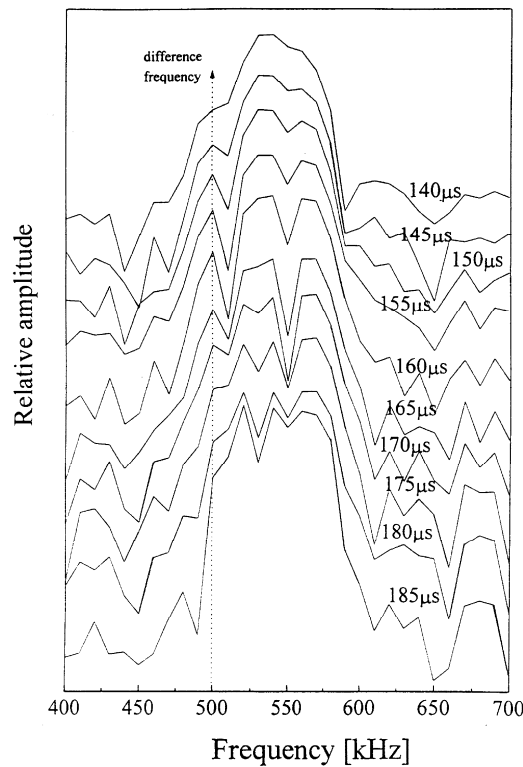


Fig.8. Spectra of reflections from the rod with crack for different time delays. Combination frequencies 570 ± 70 kHz arises only for time delays corresponding to the crack position

It is seen from Fig. 8 that the combination frequencies appear in spectra in time interval 140-175 μs that correspond to the distance to the crack. Experimentally observed spatial resolution was about 18 cm.

Another developed crack location method, i.e. the **pulse train modulation technique** [18,20] is shown in Fig. 7 (right). HF transducer emits a pulse train of short pulses of duration τ with the repetition rate F_r and the duration T_s of a sequence. Then, the nonlinear modulation can be obtained not for single pulse but rather for the entire pulse sequence. In this case the crack location and the spatial resolution are given by the same expressions as for single pulse location technique. The position of crack can be measured by strobing of receiving signal with the strobe duration equal to τ and changeable time delay. In this method the necessary condition of detection of modulation is as follows: $FT_s > 1$, which is not so strong as for single pulse location technique. From the other side the pulse train modulation technique has disadvantage - the possibility of ambiguous location due to many times reflections of each pulse from the sample ends. To avoid this problem the following relation must be satisfied $F_s < c\eta$, where η is the sound attenuation coefficient. The detection of modulation in the sequence can be done directly with the observation of modulation frequency components in the spectrum of received pulse series. The simplest case, however, is the use of the peak detector having time constant of integration larger than $1/F$. In this case the signal after detector is the sum of constant value, which is proportional to the amplitude of the received pulses and the modulation signal of frequency F , which amplitude is proportional to modulation amplitude in the received pulse sequence. With the Fourier analysis one can easily measure the modulation coefficient, which is the ratio of value of spectral component at the frequency F and the magnitude of zero-frequency component.

One of experiments was done with duraluminium rods of 210.5 cm length (Fig. 9).

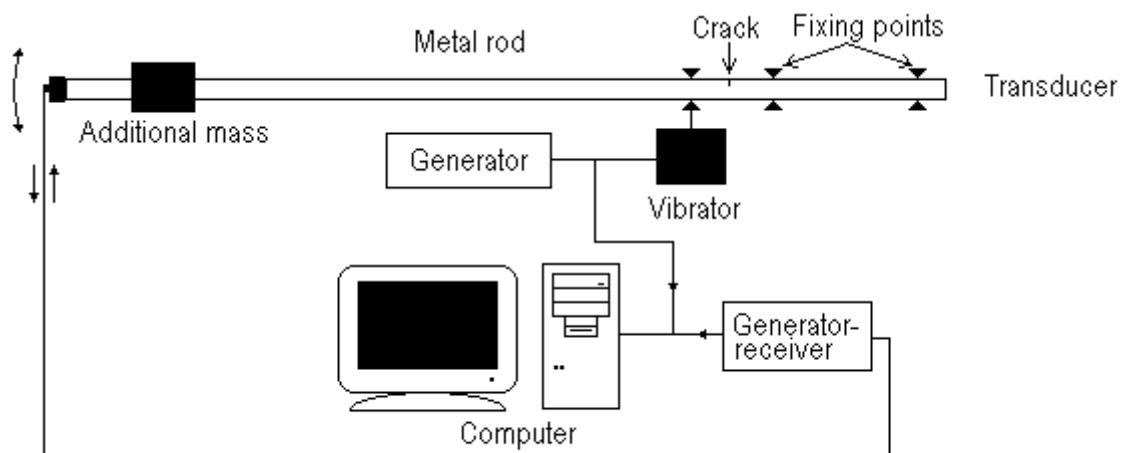


Fig.9. A scheme of the experiment on crack location with the pulse series modulation method

The transducer produced pulse train at the carrier frequency about 1 MHz with pulse duration $\tau=10 \mu\text{s}$ and the repetition period $T_r=6.5 \text{ ms}$. The spatial resolution for this experiment was about 12 mm. Low-frequency vibrations of the rod were excited by two ways - with the vibrator and with the initial displacement of the rod end from the equilibrium state. In the latter case vibrations took place at the lowest flexural mode resonance frequency of the rod. Periods T of the rod vibrations were much larger than T_r . Different kinds of artificial crack-like defects were made in several rods. A simple cut made in one of rods used as

acoustically linear defect, and a nondefected rod used as the reference one. An echogram – reflection amplitude distribution along the rod is shown in Fig.10.

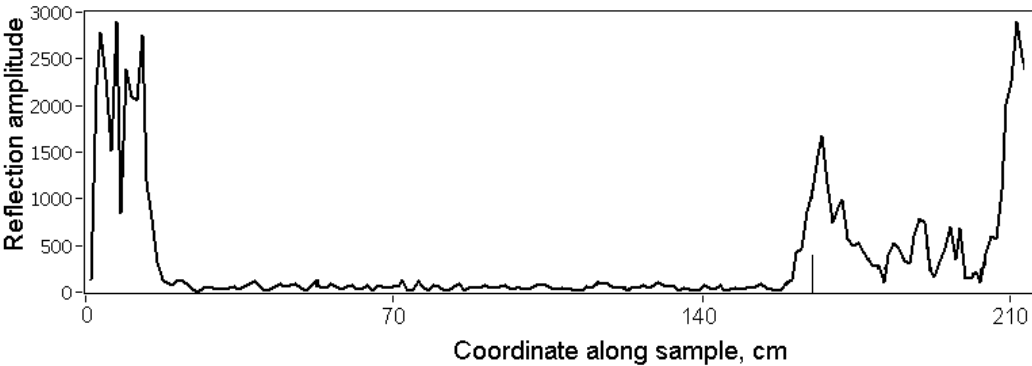


Fig.10. An echogram – distribution of the reflection amplitude along the rod. Crack position is marked by the short vertical line

Zoomed up part of this echogram around the crack is shown in Fig.11. This figure, which is the linear acoustic echogram demonstrates also the physical mechanism of the nonlinear method: the dependence of the reflection amplitude of acoustic pulses on the static deviation (0, 1.8, and 2.8 cm) of the rod end producing opening of the crack. This effect produces modulation of high-frequency acoustic wave by low-frequency vibrations. It is interesting that linear echogram obtained by averaging over the period of rod oscillations depends also on the vibration amplitudes (Fig. 12).

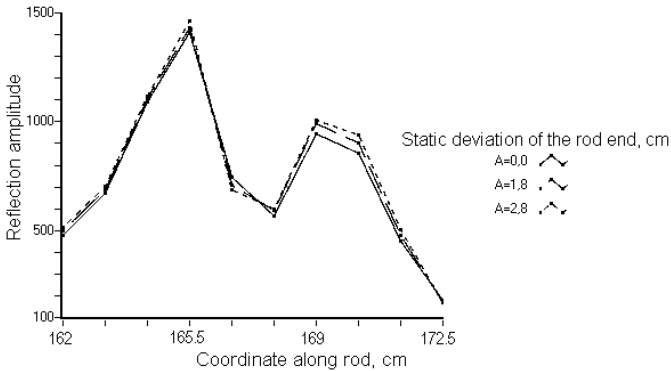


Fig.11. An echogram – distribution of the reflection amplitude along the rod

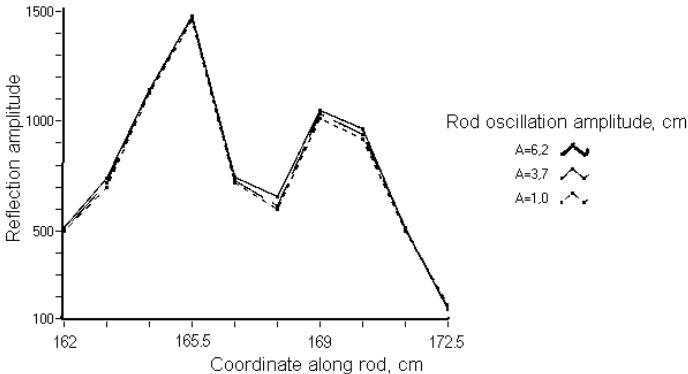


Fig.12. An echogram – distribution of the reflection amplitude along the rod

For comparison similar part of the nonlinear echogram – the distribution of the modulation coefficient along the rod around the crack is shown in Fig. 13. Different curves in figures 12 and 13 are correspond to the different oscillation amplitudes of the rod end: 1, 3.7, and 6.2 cm.



Fig.13. Nonlinear echogram – distribution of the modulation coefficient along the rod near the crack

It is seen from Figs. 11-12 that rod oscillations influence on the reflection amplitudes not only in the position of the crack (maximum in figures 11, 12 near the distance 165.5) but also at larger distances. One can see this effect in Fig. 13 for the modulation coefficient. The nature of this phenomenon is probably related with existing of different kinds of waves in the rod: the transducer generates not only longitudinal but other kinds of waves in the rod propagation with some different velocities.

The contrast between acoustically linear defect (not changing during oscillations) and crack-like defect can be enough high which allows one to indentify crack. It is demonstrated in Fig. 14. Data for this figure were obtained in similar to previous example experiment with duraluminium rods of 91 cm length. The transducer produced pulse sequence at the carrier frequency 1.2 MHz with $\tau = 20 \mu s$ and $F_r = 293 \text{ Hz}$. Low-frequency vibrations in the rod were excited with the small vibrator. A simple cut made in one rod used as acoustically linear defect, and artificial crack was made in another rod. Upper picture in Fig. 14 shows spectrum of the envelope of the pulse train reflected from the cut (acoustically linear defect), and the lower picture shows spectrum of the envelope of the pulse train reflected from the crack.

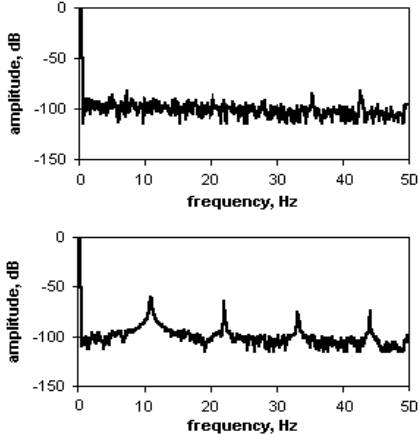


Fig. 14. Output spectra of signals obtained with the pulse sequence modulation method in rods with acoustically linear defect – cut (upper) and with the crack (lower)

One can see that the pulse train reflected from acoustically linear cut has no modulation while the sequence reflected from the crack has modulation. The modulation coefficient is about -60 dB, which is easily detectable since it is about 40 dB higher than the level of “modulation noise” that is obtained from the acoustically linear defect – cut.

3. NONLINEAR ACOUSTIC VISION OF CRACK-LIKE DEFECTS IN SOLIDS WITH THE MODE TOMOGRAPHY TECHNIQUE

The mode tomography techniques is based on the modulation method: low-frequency wave changes parameters of the high-frequency probe wave propagating through the crack, i.e. produces modulation of high-frequency wave by the low-frequency one. The modulation coefficient (index), therefore, contains information on interaction of high- and low-frequency waves at the crack. The modulation index depends on crack position relatively to nodes and antinodes of excited low-frequency oscillation modes in a sample.

Consequently, the nonlinear force, which generates the modulation frequency components act at the position of the crack. Exciting different low-frequency modes in the object one can get a set of modulation amplitude responses from the testing sample. Resonance properties of high frequency acoustic waves are usually not as strong as for low frequency oscillations, and by additional local spatial or frequency averaging the influence of those resonances on modulation indexes can be easily avoided. As a result by measurement of the modulation indexes for different low-frequency modes one can reconstruct the crack position [19, 21].

Consider this method for 1-dimensional case. It may be, for example, a rod. Low-frequency (LF) longitudinal modes in such a sample for the free-boundary conditions at both ends can be written as:

$$u_n(z, t) = A_n \cdot \sin \frac{\pi n z}{l} \cdot \cos \Omega_n t, \quad n=1, 2, 3, \dots \quad (1)$$

Here $u_n(z, t)$ is the displacement in the sample, l - the sample length, A_n - the amplitude, Ω_n - resonance frequencies of the modes. Suppose that u_ω is the displacement in a sample caused by the high-frequency (HF) wave propagating in it.

Without a crack in the sample the LF and HF waves do not interact to each other (we neglect weak interaction of waves due to normal, i.e. low-level nonlinearity of the material without crack-like defects). If there is a crack in the sample they interact producing the modulation effect, which is proportional in the approximation of the quadratic nonlinearity to the product of $u_n(z, t)$ and u_ω :

$$\tilde{u}_n = \alpha \cdot u_n(z_0) u_\omega. \quad (2)$$

Here \tilde{u}_n is the amplitude of a wave, which is generated by the nonlinear force in the crack at the combination frequency components (modulation frequency components) $\omega \pm \Omega_n$. Suppose that the newly generated high-frequency waves at the combination frequencies propagate in the sample as in infinite 1-D medium. The modulation index can be derived as:

$$M_n = \frac{1}{A_n} |\tilde{u}_n / u_\omega| = \frac{\alpha |u_n(z_0)|}{A_n}. \quad (3)$$

Then, introduce the parameter \tilde{M} as:

$$\tilde{M}(z, z_0) = \sum_n M_n \sin k_\Omega z = \alpha \cdot \sum_n |\sin k_\Omega z_0| \cdot \sin k_\Omega z, \quad (4)$$

where $k_\Omega = \pi n / l$. It can be easily seen that \tilde{M} has two peaks: one is in the position of the crack at $z = z_0$ and the second – imaginary – at $z = l - z_0$. Spatial resolution of this technique depends on the number of excited modes of flexural oscillations.

To verify the modulation mode method we carried out model 1-dimension experiments with metal strings and rods. A scheme of the first experiment is shown in Fig. 15.

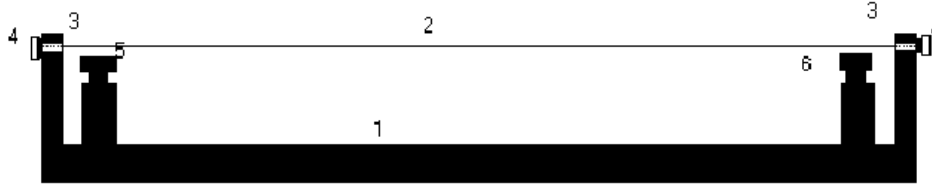


Fig.15. A scheme of the experiment with a metal string: 1 - platform, 2 – string, 3 – supports, 4 – high frequency piezoceramic acoustic transducers (one of which is the emitting and the second is the receiving), 5 – an electromagnet for excitation of transversal string oscillations, 6 – electromagnetic sensor for measurement of the transversal string oscillations

The 2-meter string was stretched between two supports fastened to a massive metal platform. Transverse string oscillations were excited with the electromagnet 5. Electromagnetic sensor 6 was used to measure amplitudes of the string transversal oscillations. Acoustic waves (~ 200 kHz) in the string were generated by a piezoceramic transducer fastened to the edge. A signal was registered by the another piezoceramic transducer at the opposite end of the string. The string was excited step by step at the mode resonance frequencies and the modulation coefficients of high-frequency wave were measured for each of the low-frequency mode resonance. Amplitudes of low-frequency modes were also measured by the electromagnetic sensor.

Experiments were done with the normal string and with a string having a small crack. A crack was made by a cut in a small drop of hard solder on the string. The experimentally obtained mode distributions of the modulation indexes for normal string and the string with a crack are shown in Fig. 16.

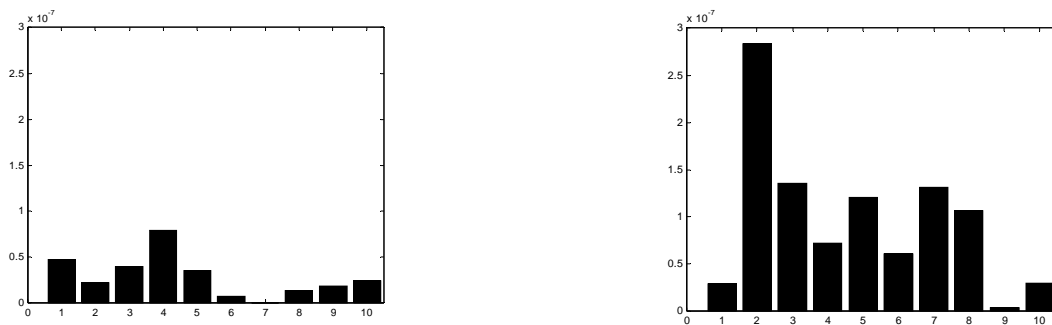


Fig.16. Modulation coefficients for different modes: normal string (left), string with a crack (right)

It is seen from the figure 16 that the string with a crack has several times higher nonlinear responses than the normal one. It is obvious that additional artificial nonlinearity is introduced in the system in points of contact of the string with the supports. Therefore the

nonlinear responses for the normal string can be considered as the background nonlinearity. One can also see that the modulation indexes are very much different for different modes which is in accordance to the theoretical model. Result of reconstruction of crack position by the use of one of algorithms is shown in Fig. 17. One can see two main peaks in Fig. 17. The relative nonlinear parameter M is maximal at the site of the crack. Left maximum in the figure is real and corresponds to the crack position while the right peak is imaginary because of the symmetry of the algorithm and the modes.

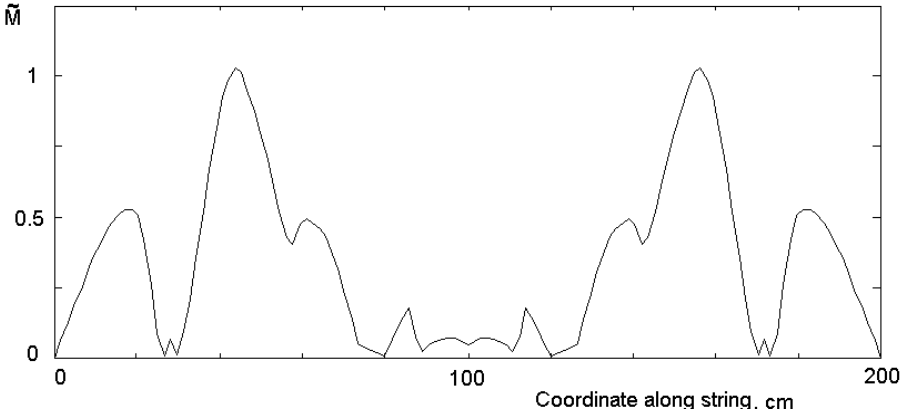


Fig.17. Reconstruction of crack position by the nonlinear modal modulation tomography method

A modified algorithm of crack location can be develop to avoid of imaginary peak at $z = l - z_0$. To this end one need to measure the mode modulation coefficients with sign (phase) [22]. Then, the modified parameter M becomes

$$M(z, z_0) = \alpha \sum_n \sin k_{\Omega} z_0 \cdot \sin k_{\Omega} z . \tag{5}$$

It has only one peak at $z=z_0$.

The modified technique was verified in experiments with metal rod. A scheme of the experiment is shown in Fig. 18. A duraluminium rod of 2.1-m length was fastened by two ropes to the support. The rod had a crack at 50 cm distance from one of ends. High-frequency piezoceramic transducer was glued to one end of the rod, and the sensor - to the another end. In this experiment the rod had free-end boundary conditions. The transducer emitted continuous longitudinal waves into the rod at the frequency about 200 kHz.

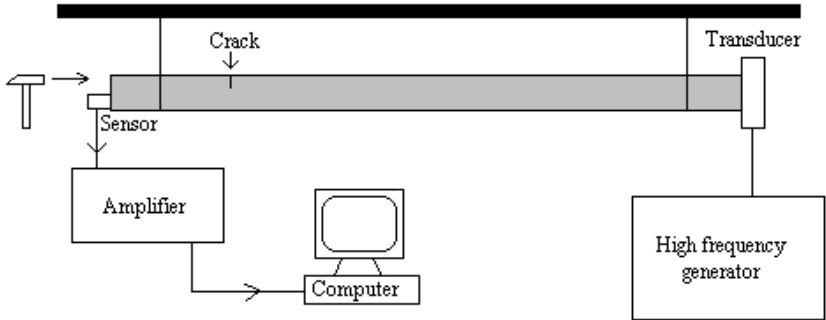


Fig.18. A scheme of the experiment

Longitudinal resonance modes were excited in the rod by the shock of hammer. They were generated simultaneously. Such a technique allows one to measure all the modulation indexes in a single experiment, as the spectrum of the registered signal contains modulation frequency components for all of the modes. For the free-end boundary conditions in the experiment with the rod longitudinal modes are described by the same functions as in equation (1).

Fig. 19 shows an oscillogram of signal registered from the sensor at the rod. It is seen high-frequency wave (constant amplitude) generated by the transducer and low-frequency decaying signal excited in the rod by a hammer.

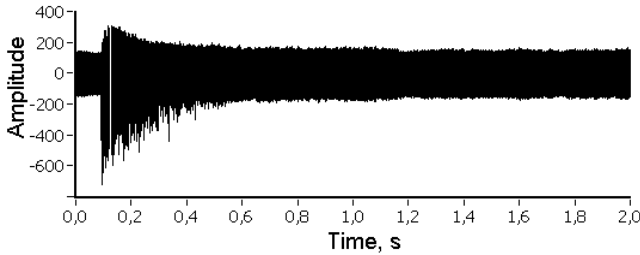


Fig. 19. An oscillogram of the high and low-frequency signals from the sensor at the rod

Hammer shock excites many modes in the rod. Selection of longitudinal modes which are of our interest was done with the Fourier analysis. Modulation coefficients for each of the mode are also obtained from the analysis of data in Fig. 19. Then by comparison of phases of envelopes of the high-frequency signal with the low-frequency oscillation for each of the mode one can get the modulation index with sign. The result is presented in Fig. 20.

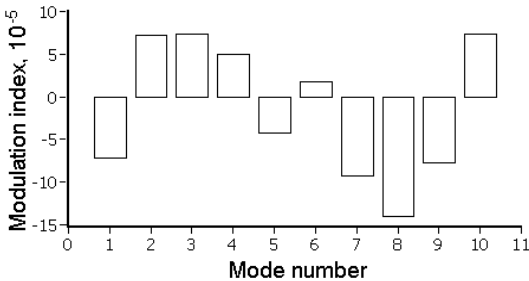


Fig.20. Modulation coefficients for different longitudinal modes in the rod, obtained with sign

Data in figure 20 allow one to find crack position. Result of reconstruction of crack position in the rod made in accordance with the equation (5) is shown in figure 21. It is in agreement with the real crack position.

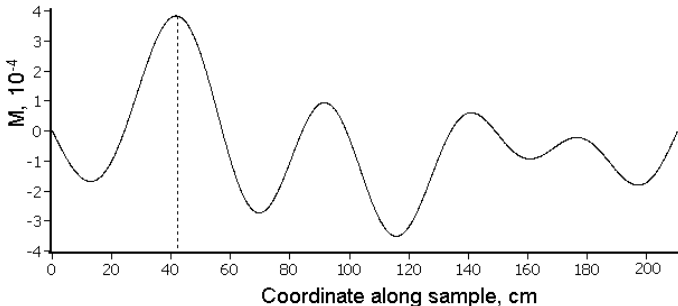


Fig.21. Reconstruction of crack position by the modified mode modulation tomography method

4. CONCLUSION

In this work we demonstrated potentialities of obtaining images of nonlinear scattering objects in acoustic fields at the difference frequency. Acoustic imaging at the difference-frequency can be an effective technique for investigating various objects. This method may be useful, for example, for acoustical observation of objects covered by gas microbubbles producing high acoustic nonlinearity at the surface of the object or bubble clouds. Spatial resolution and sharpness of the image obtained at difference-frequency waves are higher than in the case of a linearly scattered signal. The use of the difference-frequency scattering for diagnostics of nonlinear targets is effective due to low level of reverberation at the difference frequency and due to high sensitivity of the nonlinear scattered wave spectrum to the variation of diagnostic parameters.

We described also the nonlinear acoustic techniques for observation of cracks in solids. Acoustic echo-pulse techniques are relatively simple and can be used with the traditional linear acoustic echo method. But high-frequency acoustic pulses decay rapidly in many materials: concrete, composites, etc. where those methods hardly be used. An alternative technique is the mode modulation tomography. It allows one to reconstruct crack position basing on measurements of the modulation indexes for resonance low-frequency modes in the sample. This method was successfully verified in experiments. It can be prospective tool for nondestructive testing of different materials and constructions.

This work was supported in part by the Russian foundation for basic research.

REFERENCES

- [1] E. Zabolotskaya, S. Soluyan, Emission of harmonic and combination frequency waves by air bubbles, *Sov. Acoust. Phys.*, Vol.18, 396-398, 1972.
- [2] Eller, H. Flynn, Generation of subharmonics of order one-half by bubbles in a sound field, *J. Acoust. Soc. Am.*, Vol.46, 722-727, 1969.
- [3] L. Ostrovsky, A. Sutin, Nonlinear acoustic diagnostics of discrete inhomogeneities in liquids and solids, *Proc. 11th Int. Congr. Acoust.*, Vol.2, 137-140, Paris, 1983.
- [4] V. Zverev, Yu. Kobelev, D. Selivanovsky, A. Sokolov, On a method of detection of gas bubbles in a liquid, *Sov. Tech. Phys.* Vol.50, 1544-1545, 1980.
- [5] T. Leighton, A. Walton, J. Field, Acoustic bubble sizing by combination of subharmonic emission with imaging frequency, *Ultrasonics*, Vol.29, 319-323, 1991.
- [6] I.N. Didenkulov, S.W. Yoon, A. Sutin, E.J. Kim, Nonlinear acoustic Doppler effect and its use for bubble flow velocity measurement, *J. Acoust. Soc. Am.*, Vol.106, 2431-2435, 1999.
- [7] I. Didenkulov, L. Kustov, A. Martyanov, P. Vyugin The difference-frequency acoustic scattering from nonlinear objects, *Hydroacoustics*, Vol.9, P.31-38, 2006.
- [8] O. Buck, W.L. Morris, J.N. Richardson, Acoustic harmonic generation at unbonded interfaces and fatigue cracks, *Appl. Phys. Lett.*, Vol.33, 371-373, 1978.
- [9] V.A. Antonets, D.M. Donskoy, A.M. Sutin, Nonlinear vibrodiagnostics of delayer in layer construction," *J. Mech. Composit. Materials*, Vol.5, 934-937, 1986.
- [10] G.D. Meegan, P.A. Johnson, R.A. Guer, K.R. McCall, Observations of nonlinear elastic wave behavior in sandstone, *J. Acoust. Soc. Am.* Vol.94, 3387-3391, 1993.
- [11] A. Korotkov, A. Sutin Modulation of ultrasound by vibrations in metal constructions with cracks, *Acoustics Letters*, Vol.18. P.59-62, 1994.
- [12] A.M. Sutin, V.E. Nazarov, Nonlinear acoustic methods of crack diagnostics, *Radiophysics & Quantum Electronics*, Vol.38, P.109-120, 1995.

- [13] A.M. Sutin, A.S. Korotkov, I.N. Didenkulov, E.J. Kim, S.W. Yoon, Nonlinear acoustic methods for crack and fatigue detection, Proc. of Physical Acoustics Workshop "Safety diagnostics of Underwater Constructions by Using Acoustics", KAIST, Seoul, Korea, P.43–55, 1995.
- [14] I.N. Didenkulov, A.E. Ekimov, V.V. Kazakov, Nonlinear interaction of torsional and flexural waves in a rod with a cracklike defect, Acoustical Physics, Vol.43, P.462-468, 1998.
- [15] A. Ekimov, I. Didenkulov, V. Kazakov Modulation of torsional waves in a rod with a crack, J. Acoust. Soc. Am., Vol.106, P.1289-1292, 1999.
- [16] I.N. Didenkulov, A.M. Sutin, A.E. Ekimov, V.V. Kazakov, Interaction of sound and vibrations in concrete with cracks, Nonlinear Acoustics at the turn of the Millenium, Melville, New York, P.279-282, 2000.
- [17] J.P. Kim, E.J. Kim, S.W. Yoon, A.M. Sutin, Nonlinear acoustic modulation technique for nondestructive flaw detection, J. Acoust. Soc. Am., Vol.101, P.3029-3030, 1997.
- [18] I.N. Didenkulov, A.M. Sutin, V.V. Kazakov, A.E. Ekimov, S.W. Yoon Nonlinear acoustic technique of crack location, In: W.Lauterborn and T.Kurz (eds.), Nonlinear Acoustics at the turn of the Millenium, Melville, New York, P.329-332, 2000.
- [19] I.N. Didenkulov, N.V. Kurochkin, A.A. Stromkov, V.V. Chernov Modulation modal method for crack location, In: Proc. of the 10-th Int. Congress on Sound and Vibration. IIAV, Stockholm, Sweden, P.3565-3572, 2003.
- [20] I.N. Didenkulov, M.V. Martyshev, S.I. Muyakshin, Nonlinear acoustic location of cracks, Vestnik of Nizhny Novgorod State University, Ser. "Radiophysics", Vol.1(4), P.41-50, 2006.
- [21] I.N. Didenkulov, S.W. Yoon Nonlinear acoustic modulation methods for NDE. In: CD Proc. 9-th Intern. Conf. WESPAC-IX, Seoul, Korea, p.472/1-8, 2006.
- [22] I.N. Didenkulov, M.V. Martyshev Investigation of the method of the nonlinear modulation mode tomography of cracks, In: Proc. XIX session of the Russian Acoust. Soc., Vol.1, P.118-121, Moscow, GEOS, 2007.